Check for updates

Formulation of a fast 2D urban pluvial flood model using a cellular automata approach

Bidur Ghimire, Albert S. Chen, Michele Guidolin, Edward C. Keedwell, Slobodan Djordjević and Dragan A. Savić

ABSTRACT

With the increase in frequency and severity of flash flood events in major cities around the world, the infrastructure and people living in those urban areas are exposed continuously to high risk levels of pluvial flooding. The situation is likely to be exacerbated by the potential impact of future climate change. A fast flood model could be very useful for flood risk analysis. One-dimensional (1D) models provide limited information about the flow dynamics whereas two-dimensional (2D) models require substantial computational time and cost, a factor that limits their use. This paper presents an alternative approach using cellular automata (CA) for 2D modelling. The model uses regular grid cells as a discrete space for the CA setup and applies generic rules to local neighbourhood cells to simulate the spatio-temporal evolution of pluvial flooding. The proposed CA model is applied to a hypothetical terrain and a real urban area. The synchronous state updating rule and inherent nature of the proposed model contributes to a great reduction in computational time. The results are compared with a hydraulic model and good agreement is found between the two models.

Key words | cellular automata, local rules, parallelization, pluvial flood inundation

Bidur Ghimire
Albert S. Chen (corresponding author)
Michele Guidolin
Edward C. Keedwell
Slobodan Djordjević
Dragan A. Savić
Centre for Water Systems,
College of Engineering Mathematics & Physical Sciences,
University of Exeter, Exeter,
EX4 4QF,
UK
E-mail: *A.S.Chen@exeter.ac.uk*

ABBREVIATIONS AND NOTATIONS

1D	One-dimensional
2D	Two-dimensional
BCR	Building Coverage Ratio
CA	Cellular Automata
CAESAR	CA Evolutionary Slope and River
CFL	Courant–Friedrichs–Lewy condition
CRFs	Conveyance Reduction Factors
DEM	Digital Elevation Model
GPU	Graphical Processing Unit
IZs	Impact Zones
LGCA	Lattice Gas CA
LiDAR	Light Detection and Ranging
NH	Neighbourhood
UIM	Urban Inundation Model
A	Cell area (m^2)
A_c	Cell area of the central cell (m^2)
A_k	Cell area of cell with rank k (m^2)
d	Water depth (m)
d_c	Water depth of the central cell (m)
F	Flux volume being transferred between two cells (m^3)
g	Gravitational acceleration (m/s^2)
i	Index of layer for receiving water from the central cell in a local neighbourhood
j	Index of cell
k	Index of cell rank
L_i	The ith layer to receive water from the central cell in a local neighbourhood
n	Manning's roughness coefficient
R	Hydraulic radius (m)
r	Rank of a cell
r_c	Rank for the central cell in a local neighbourhood
S	Water surface gradient
t	Computing time (s)

doi: 10.2166/hydro.2012.245

Downloaded from http://iwaponline.com/jh/article-pdf/15/3/676/387056/676.pdf
by guest

θ	Non-dimensional flow relaxation parameter
V_c	Water volume of the central cell ($=A_c.d_c$)
v	Corrected flow velocity between cells (m/s)
v^*	Flow velocity between cells calculated before correction (m/s)
WL	Water level elevation (m)
z	Ground elevation (m)
Δt	Size of a time step (s)
ΔV_i	Volume to be distributed to layer i from the central cell (m^3)
ΔV_k	Volume transferred to layer k from the central cell (m^3)
ΔWL_i	Difference of water surface levels between cells ranked i and $i+1$ (m)
Δx	Distance between the centres of two adjacent cells (m)

INTRODUCTION

Urban flood modelling often involves the use of computational techniques to simulate the spread of water onto a wide surface area that contains complex urban features. These techniques are applied mainly to solve physically based flow governing equations: conservation of mass, momentum and energy. Data-driven models and empirical stochastic models employing probabilistic approaches to predict flood extents are also used (Chang *et al.* 2010). Due to the complexity of the urban setup and infrastructure, fast and accurate urban flood modelling has always been a challenging task. Many two-dimensional (2D) models (Nguyen *et al.* 2006; Hunter *et al.* 2008; Chen *et al.* 2010) have been developed to simulate urban flooding, although their complexity, computational cost and significant data requirements limit their efficient application to wide areas.

Various approaches have attempted to reduce the computational time of 2D flood modelling. Some models divided the overland flow area into a series of ponds and connecting pathways and implement a one-dimensional (1D)–1D approach to simulate urban floods. Lhomme *et al.* (2008) proposed a rapid flood spreading method that divides the domain into various impact zones (IZs) consisting of accumulation points and communication points where the transfer of water takes place. The method splits and merges IZs as the spatio-temporal evolution of inundation proceeds. Maksimović *et al.* (2009) developed a model that creates the overland flow pathway network automatically based on topography, so that the coupled 1D sewer and 1D surface flow models can be applied to dual-drainage simulation. Vojinovic & Tutulic (2009) proposed a method in which building elevations are raised and road surfaces are lowered to model urban floods. Chen *et al.* (2012a) introduced the building coverage ratio (BCR) and the conveyance reduction factors (CRFs) in the urban inundation model (UIM) to retain the detailed features in 2D coarse-grid modelling, so that simulation time can be reduced without losing the accuracy of modelling results. Chen *et al.* (2012b) further developed a multi-layered approach in the UIM to improve the accuracy of coarse-grid modelling.

These approaches required considerable pre-processing effort to extract the key information from the detailed terrain and building features to such an extent that parallelization of computing processes has become another solution to speed up the computing of 2D models. Lamb *et al.* (2009) implemented massive parallelization using graphical processing units (GPUs) in the JFLOW-GPU to reduce the computational time. Neal *et al.* (2009) adopted OPEN-MP and improved the performance of the LISFLOOD-FP significantly. Judi *et al.* (2011) applied Java multithreading and domain-tracking techniques to achieve faster 2D inundation modelling.

Cellular automata (CAs) are computational methods based on the simulation of a discrete space in which a set of universal laws apply. They were conceived in the 1940s by John von Neumann and Stan Ulam. The CA method was originally treated as a curiosity, but in recent years the approach has been shown to work effectively for the fast simulation of physical systems in the biological and physical sciences (Ermentrout & Edelstein-Keshet 1993; Ilachinski 2001). A cellular automaton is composed of a lattice of cells that adopts one state from a (usually finite) set. The automaton runs by executing a set of universal state transition rules on the lattice, changing the states of cells in discrete time steps. CA have been found to be powerful techniques due to their ability to discretise time and space and thus reduce the computational overhead associated with the computation based on solving hydraulic equations.

Downloaded from http://iwaponline.com/jh/article-pdf/15/3/676/387056/676.pdf
by guest

Thomas & Nicholas (2002) applied a CA model to simulate braided river flow by routing the flow from the cell under consideration into five downstream cells. Coulthard *et al.* (2002) developed the CA Evolutionary Slope and River (CAESAR) model to simulate the sediment evolution along river channels. Although accurate, the four-sweep scanning algorithm employed in CAESAR impacts on its performance to such an extent that the model efficiency cannot be assured. A Lattice Gas CA (LGCA) simulation model (Judice *et al.* 2008) was employed in real-time computer games using GPU computation. In such an approach, macroscopic density and velocity of particles define the new fluid configuration. Krupka *et al.* (2007) adopted a concept similar to CA that uses three states of a cell (dry, active and inactive) to develop a rapid inundation model. However, the model can only determine the final inundation extent because of the lack of dynamic spreading. The stability criteria in storage cell and diffusion models like LISFLOOD-FP (Hunter *et al.* 2005) often require smaller time steps, when high resolution grids are used, than the full 2D shallow-water equation models. More recently, Dottori & Todini (2011) employed a modified local time-step algorithm to improve the performance of their original CA model that had employed Manning's formula for the computation of interfacial discharges between computing cells. Although the model was called a CA model, it was similar to the storage cell models, such as the LISFLOOD-FP model, neglecting both local and advective inertial terms in the momentum equations. In fact, Manning's resistance formula was used to calculate intercellular flux rates.

This paper describes a novel reduced-complexity model for fast and accurate urban flood simulations, based on the CA approach, to evaluate flood risk more efficiently for a large number of model runs, which existing hydraulic models have difficulty in dealing with. We developed the CA pluvial flood model in which the spatio-temporal variations in flood depth and velocity are governed by local rules in the neighbourhood (NH). The model was applied to two case studies to analyse the dynamics of the propagation of flood water over terrain due to a storm event. Results were compared with that of the UIM to assess the performance of the CA model. The UIM is a 2D non-inertia model derived from the Saint Venant equations in which the inertial terms are neglected by the assumption that the acceleration terms of water flow on the land surface are relatively small compared with gravity and friction terms (Chen *et al.* 2007). The alternating direction explicit (ADE) finite difference numerical scheme is applied to solve the equations on a regular grid (Hsu *et al.* 2000). The stability of the scheme is ensured by checking the Courant condition in every time step and choosing the computational time step accordingly.

CA FORMULATION

The proposed model consists of five essential features of a true cellular automaton: a discrete space, neighbourhood, cell state, discrete time step and a transition rule (Itami 1994). The square grid digital elevation model (DEM) provides the discrete space for the CA set up. The NH chosen consists of the central cell itself and its four cardinal adjacent cells totalling five cells, called the von Neumann type NH (an alternative being the Moore NH, consisting of eight surrounding cells and the central cell). To implement this, the von Neumann type NH is chosen and other NH types will be tested in the future for their suitability. The effective rainfall lands directly on the whole area of the terrain being considered. Hydrological losses are not considered in the model at this stage. The movement of water is mainly driven by the slopes between cells and limited by the transferrable volume and the hydraulic equations. The transferrable volume is the minimum of the total volume within the giving cell and the space available in the receiving cells. Manning's equation and the critical flow equation are applied to restrict the flow velocity. The assumption is that the water can only propagate from one cell to its NH cells, according to the hydraulic gradients, in one computing time step.

In the calculation, NH cells are ranked according to the water level, as 1 for the cell with the lowest level and 5 for the highest one, to determine the direction of flow between cells. Only the outflow fluxes from the central cell to its neighbours with lower ranks are calculated. Any inflow to the cell under consideration is eventually calculated as the outflow from its neighbour that has a higher water level

Downloaded from http://iwaponline.com/jh/article-pdf/15/3/676/387056/676.pdf
by guest

on the opposite of the cell interface. The fluxes through the interfaces of the central cell are determined by the states of NH cells in previous time steps and stored as intermediate buffers for updating the states of cells. The states of flood depths of all cells are updated simultaneously when all interface fluxes are determined. The main algorithm implemented is as follows:

Main algorithm

Program start

1. Initialization of variables (depth, water surface elevation) and data input (terrain, rainfall)

2. Start of time loop {

3. Add precipitation depth directly to the water depth on the cells

4. Computation starts in the local NH {

i. Ascending cell ranking based on the water surface elevations

ii. Layer-wise calculation of outflows from central cell

iii. Distribution of layer-wise fluxes within the NH

iv. Calculate cell interfacial velocities

5. End of local NH loop}

6. Determine time step Δt required for the distributions applied

7. Update simulation time: $t = t + \Delta t$

8. Update the states (depths, water surface elevation) for new time step

9. Apply boundary conditions to suit the flow conditions

10. Data outputs for visualization and analysis

11. Repeat until the end of simulation time

12. End of time loop}

Program end

Outflow flux calculation

The calculation process starts with cell ranking, based on the water surface elevation, in the local NH with five discrete states of cell ranks $\{r = 1, 2, 3, 4, 5\}$. Figure 1(a) shows that the space between the water levels of cells is divided into four layers. L_i is the free space between the water levels of cells ranked i and $i+1$ that can accommodate the water volume from cells with higher ranks. If the rank of the central cell is r_c (e.g. rank 3 as shown in Figure 1(b)), there will be r_c–1 number of cells receiving water as flux through the NH cell boundaries. In the distribution among

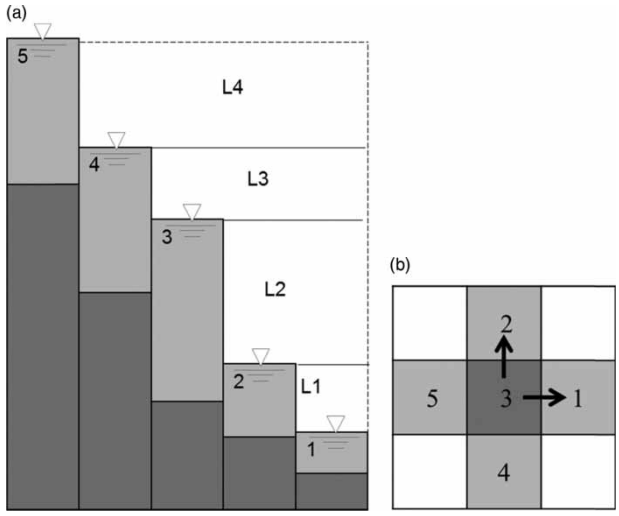

Figure 1 | (a) Cells ordered in NH according to their ranks, L1–L4 are layers of free spaces between the water levels of two cells that are available within NH for water distribution, the numbers shown are cell ranks. In this diagram the ground level for each cell is shown in dark grey and the water level light grey, (b) an example of outflow fluxes (shown by arrows) from the central cell having rank 3 to its neighbouring cells.

layers, there will be at most r_c–1 layers to receive water, if enough water is available in the central cell. Thus outflow volume to the layer i can be given by the following formula that is applied locally for each cell considered:

$$\Delta V_i = \min\left\{ V_c - \sum_{k=1}^{i-1} \Delta V_k, \Delta WL_i \sum_{k=1}^{i} A_k \right\} \quad (1)$$

where V_c is the water volume of the central cell in the previous time step; ΔV_k is the volume distributed to layer k, $\sum_{k=1}^{i-1} \Delta V_k$ the total volume has been distributed to layers 1 to $i-1$; $V_c - \sum_{k=1}^{i-1} \Delta V_k$ represents the remaining volume available for distributing to layer i after filling i–1 layers. $\sum_{k=1}^{i} A_k$ is the total surface area of layer i; ΔWL_i is the water level difference between cells ranked i and $i+1$; $\Delta WL_i \sum_{k=1}^{i} A_k$ is the available space for storage in layer i. For the layer adjacent to the central cell, an additional term

$$\sum_{k=1}^{i} A_k / A_c + \sum_{k=1}^{i} A_k \left(V_c - \sum_{k=1}^{i-1} \Delta V_k \right)$$

is applied to limit ΔV_i, which assumes that the water levels for all cells will reach an equivalent level. Thus, a cell with rank r receives water only from cells with higher ranks and the water received is added on top of its own water

Downloaded from http://iwaponline.com/jh/article-pdf/15/3/676/387056/676.pdf
by guest

level. Thus the total outflow flux from the central cell to neighbouring cell with rank i is calculated as:

$$F_i = \sum_{k=i}^{r_c-1} \frac{\Delta V_k}{k} \tag{2}$$

For a regular grid, the areas of the central cell, A_c and the neighbouring cells, A_k, are constant over the domain. However, the methodology is applicable to different grid settings. Therefore, a cell containing buildings that do not allow water to flow in can be described using a variable cell area to reflect the reduced space occupied by buildings.

Depth updating

A very important step in the CA approach is the execution of the state transition rule. In the present CA calculations, the global continuous state is the flow depth in a grid cell, which is updated for every new time step. This is done by algebraically summing the water depth from all its four neighbours. The following transition rule is used to update the flow depth:

$$d^{t+\Delta t} = d^t + \theta \frac{\sum F}{A} \tag{3}$$

where, θ is a non-dimensional flow relaxation parameter that can take values between 0 and 1, F is the total volume transferred to the cell under consideration as calculated from Equation (2) and A is the cell area. The purpose of the relaxation parameter is to damp oscillations that would appear otherwise. The effect of the relaxation parameter does not impart any effect on mass conservation rather it makes the flow smooth and gradual. The values of θ are determined by numerical experiments and calibration.

Time-step calculation

For most 2D hydraulic modelling, higher resolution DEM data are being used, the required time steps will be shorter to ensure the stability of model computations, which often leads to large computational burden, such that many studies have been focused on reducing the computational time of simulations. The time increment, determined as the largest that satisfies the stability criteria anywhere in the whole domain, implies that for most of the cells only a fraction of the locally allowable time steps is used to integrate the solution in time. This represents a waste of computational effort (Zhang *et al.* 1994) and limits the use of the method. A spatially varying time step can increase solution accuracy and reduce computer run time (Wright *et al.* 1999; Crossley *et al.* 2003). In this implementation we use maximum permissible velocity which ensures the minimum time steps required to distribute the applied flux. The interfacial velocity v^* is determined based on the flux transferred through a cell boundary given by:

$$v^* = \frac{F}{d^* \Delta x \Delta t} \tag{4}$$

where, d^* is the water depth of flow available at the interface, which is the difference between higher water level and higher ground elevation of the central cell and its neighbour cell to the interface

$$d^* = \max\{WL_C, WL_N\} - \max\{z_C, z_N\} \tag{5}$$

where, WL and z are the water level and ground elevation respectively and the subscripts C and N represent central and neighbouring cells respectively.

To prevent the velocity from overshooting, a cap on the local allowable velocity is applied as given by Equation (6) based on the Manning's formula and critical flow condition as:

$$v = \min\left\{\frac{1}{n} R^{\frac{2}{3}} S^{\frac{1}{2}}, \sqrt{gd}\right\} \tag{6}$$

where, the hydraulic radius R is taken to be equal to the water depth d and S is the slope of water surface elevation and is always positive for outflow calculation. If v is less than v^*, the interfacial flux F is recalculated by replacing v^* with v in Equation (4).

The global time step is then calculated based on the global maximum velocity to satisfy the conventional

Downloaded from http://iwaponline.com/jh/article-pdf/15/3/676/387056/676.pdf
by guest

CFL criteria. Therefore, each time the state transition rule is applied, the global time step is updated using maximum velocity calculated from all cell interfaces, as given by

$$\Delta t = \frac{\Delta x}{\max\{v_j\}} \tag{7}$$

where v_j is the velocity calculated for jth cell interface for the entire domain.

MODEL TEST CASES

The model we developed has been applied to two case studies: a hypothetical terrain case and a real-world case study in the area of Keighley, UK. The hypothetical terrain consists of 30 by 20 cells with a cell resolution of 50 m, whereas the Keighley area consists of 377 by 269 cells with a cell resolution of 2 m. The excess rainfall was directly applied over the surface of the catchment uniformly in both case studies.

Hypothetical terrain

The model was tested on a hypothetical terrain shown in Figure 2. The terrain consists of both forward and reverse slopes of 0.2%. It also has a lateral slope of 0.1% toward the outlet. No flow is allowed across boundaries, i.e., the flow domain is enclosed by impervious boundaries, except for the outlet at the lowest end of the terrain. A uniform rainfall with constant intensity 20 mm/h and 1 h duration was fed to the whole terrain. A constant value of Manning's coefficient, $n = 0.01$ was applied to all cells.

Extra cells were added next to the boundary cells so that the generic rules could be applied to all the computational cells within the domain. Flows into these cells were disregarded when the open-boundary condition was applied; for closed boundary condition, an extremely high value was set for the terrain elevations of these extra cells to prevent flow moving out of the boundary. For the outflow cell a surface elevation gradient was maintained to ensure the continuity of flow.

Keighley area

An urban area at Stockbridge, Keighley in the UK was chosen (Figure 3) as a case study. An effective rainfall of intensity 42.3 mm/h was applied over the terrain, which corresponds to 100-year return period with 1-h storm duration calculated according to the Wallingford Procedure (Department of Environment 1981). As the East and the North boundaries of the area were enclosed by streams and similarly the South and the West boundaries were enclosed by roads, the entire boundary of the study area was assumed

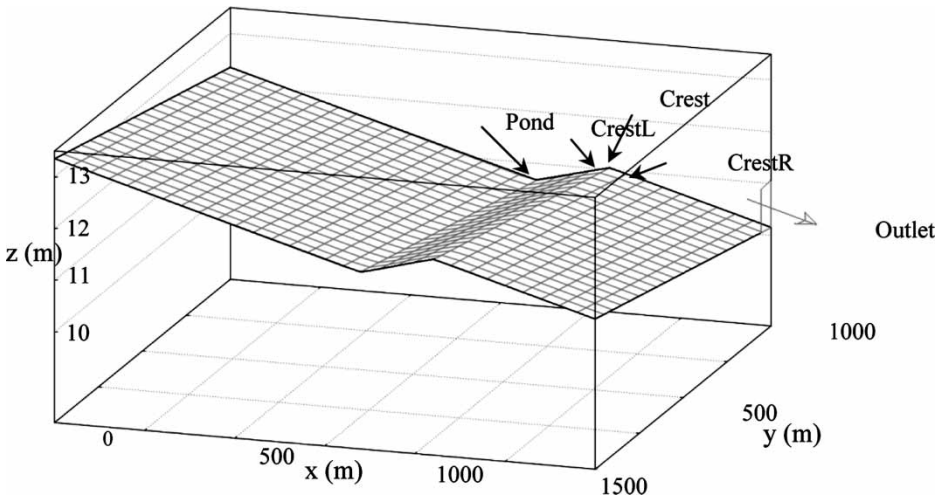

Figure 2 | Hypothetical terrain.

Downloaded from http://iwaponline.com/jh/article-pdf/15/3/676/387056/676.pdf
by guest

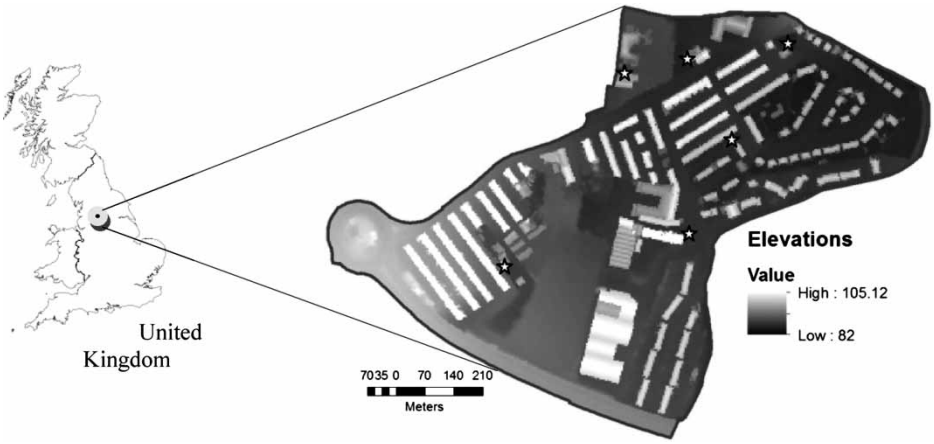

Figure 3 | Study area: Stockbridge Keighley with sample points (1–6) shown.

to be an open type, i.e. water is free to move out if the topography allows. A DEM of 2 m resolution, obtained from LiDAR, was used for topographical representation which serves as the computing grid for the CA. It was assumed that no flooding came from the river. The flood depths obtained from the proposed CA model were compared with those from the UIM to assess the CA model's performance.

RESULTS AND DISCUSSION

Hypothetical terrain

The snapshots of flood depth at selected timings are shown in Figure 4. The runoff flowed northward along the steepest slope and accumulated in the pond area. The drying and wetting processes during this spatio-temporal flow evolution

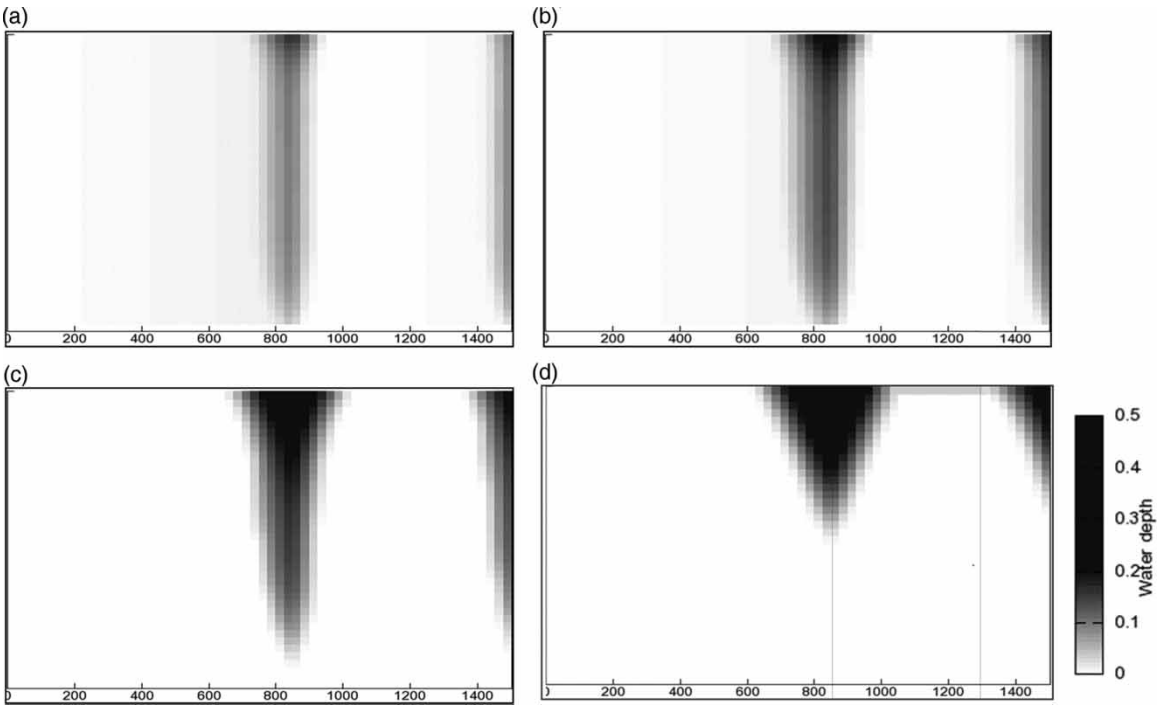

Figure 4 | Depth profiles after the onset of rainfall at (a) 40; (b) 60; (c) 100; and (d) 200 min.

Downloaded from http://iwaponline.com/jh/article-pdf/15/3/676/387056/676.pdf
by guest

were reproduced in a manner one would expect. It can also be observed that the water exchange between the two pond areas took place through the narrow strip on the lower side of the area.

The water depth hydrographs computed by both UIM and CA models at various check points are compared in Figure 5. Figure 5(a) shows the hydrographs at the point labelled as 'Pond' in Figure 2. The depth increased rapidly at the beginning (after the onset of rainfall), but when water started transferring to the downstream sub-catchment through the crest, the water depth became lower and then remained almost constant. Nonetheless, some discrepancies occurred at the later time stage due to the tendency of the CA model to release water quickly from higher elevation areas. The variation of flow depths at other points are shown in Figures 5(b)–5(d). The plots show the depths at the crest cell and its left and right cells. The CA model results at these points show a smoother variation than UIM results. This is attributed to the use of a flow relaxation parameter, which was taken as 0.7 for this implementation. The overall CA model results are in good agreement with that of UIM model. When compared with the computational speed, the CA model is almost 30 times faster than the UIM.

Keighley area

The overall results obtained from the UIM and the CA model for maximum inundation depth show very good agreement (Figure 6). Higher inundation depths can be observed along the low lying areas, which was mainly due to the accumulation of water from higher ground. The extent and pattern of maximum inundation depth are similar in both the model results. Six points (Point 1 to Point 6 in Figure 3) were carefully selected so as to represent the different flow dynamics with respect to both space and time. The temporal variation of inundation depths at the selected points are shown in Figure 7. For Points 1 and 3 (Figures 7(a) and 7(c)), the CA results were marginally higher than the UIM results after the peak depth occurs. The later horizontal portion of the plot indicated that the chosen sample points are local pond cells. For Points 2 and 5 (Figures 7(b) and 7(e)), the temporal variations of depths are in good

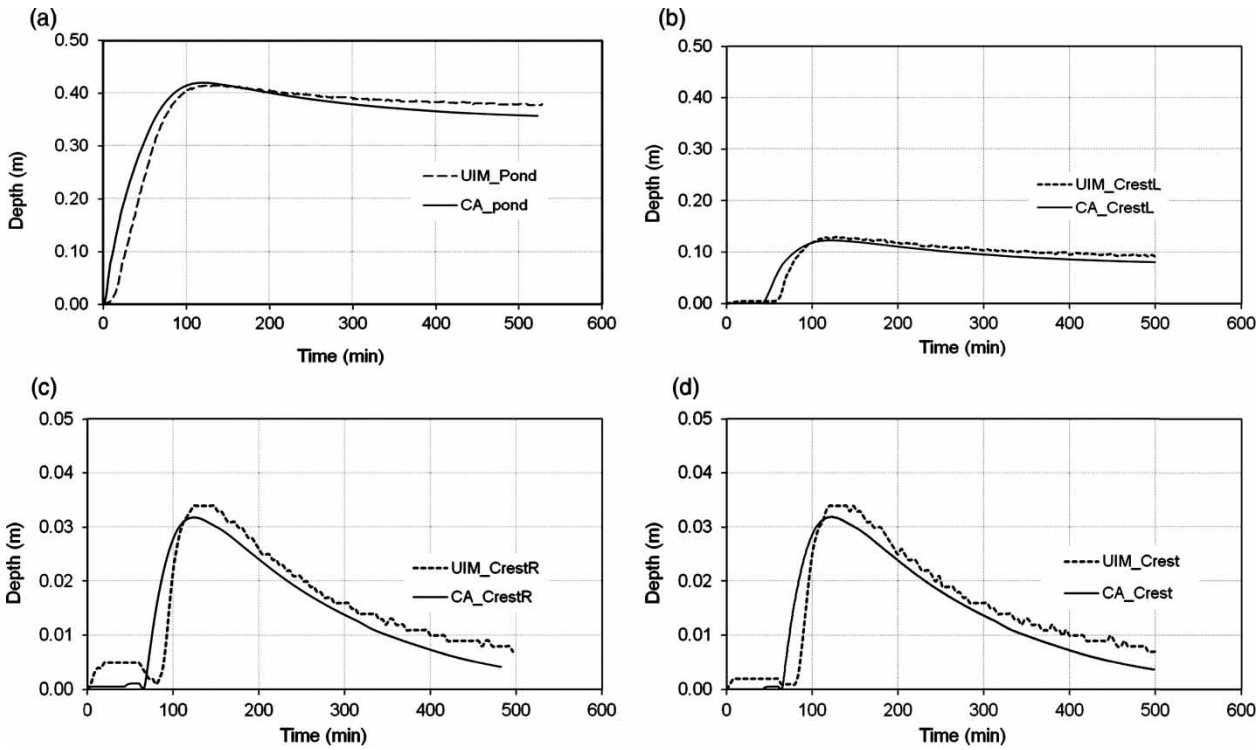

Figure 5 | Temporal variation of water depth at (a) pond; (b) left of crest; (c) right of crest; and (d) crest points.

Downloaded from http://iwaponline.com/jh/article-pdf/15/3/676/387056/676.pdf
by guest

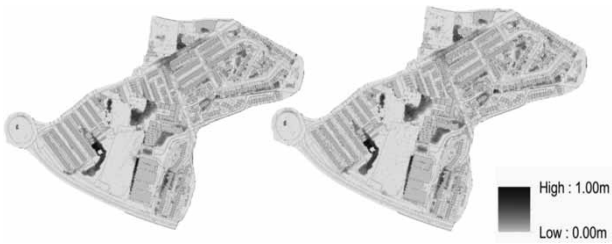

Figure 6 | Maximum inundation depth: UIM result (left) and CA result (right).

agreement for both filling and emptying periods. Points 2 and 5 are small ditch points lying on the flow paths so that a remaining depth was recorded after the peak. The results for Points 4 and 6 (Figures 7(d) and (f)), show both rising and falling limbs owing to the fact that these points are the points on the flow path. The plots show some discrepancies, however the model captures the dynamics of both build-up and subsidence of the flow depths very well. It can also be seen from the plots that the CA results are smoother than the UIM results because the relaxation parameters used in the CA damped the flow rate thereby giving slightly higher values for the flow depths for pond points. These results show a promising capability of the CA model to represent the flow dynamics in the inundation process. The computation time for the CA is much smaller than it is for the UIM. For the results shown here, the CA required approximately 3 min of processing time whereas

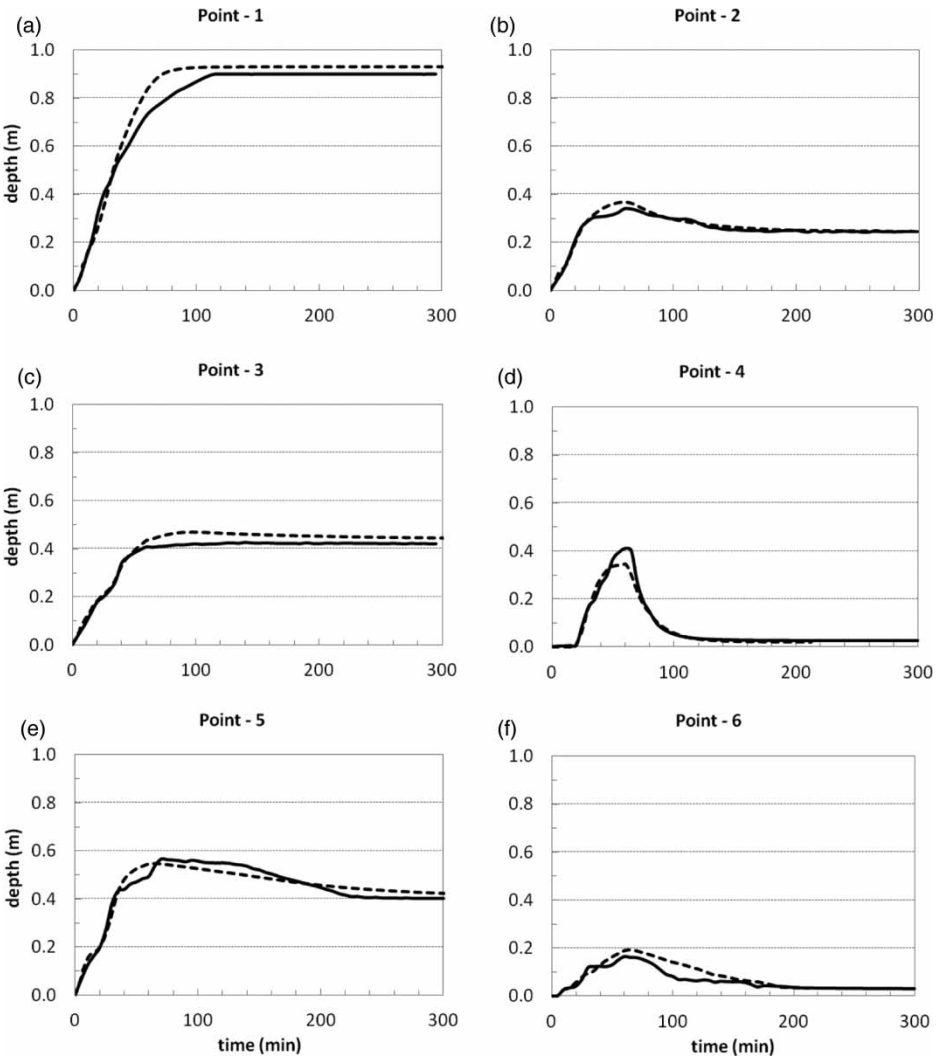

Figure 7 | Temporal variation of depths at various points from UIM (solid line) and CA (dotted lane).

Downloaded from http://iwaponline.com/jh/article-pdf/15/3/676/387056/676.pdf
by guest

the UIM required 98 min of processing time on a desktop computer (Intel Pentium D CPU 3 GHz, 1 GB of RAM). The root mean square error (RMSE) calculated for maximum depths over the domain, assuming the UIM results as a reference, was as small as 0.015 m.

CONCLUSION

The proposed 2D CA model has been applied to a hypothetical terrain and an urban area. Numerical results obtained were compared with those of a physically based model UIM that employs Saint Venant's equations. The depth hydrographs obtained at various check points for the hypothetical terrain show consistent results to the UIM, which demonstrates the CA model's capability to simulate the spatio-temporal evolution of runoff. It captured the dynamics of wetting and drying over the terrain well. In the case of Keighley, the results for maximum inundation depths show a good agreement between the CA and the UIM results. The comparisons of depth hydrographs at various sampling points also show a consistent spatio-temporal evolution of the inundation process. The state updating algorithm strongly contributes to the reduction of computational time due to the straightforward algorithm to distribute water in the NH, thereby avoiding the computation of a time consuming iterative solution which would have been incurred in hydraulic models based on partial differential equations. In both the cases mentioned above, the CA model run times were over 30 times shorter than that for the UIM for no significant discrepancies in the results. One can expect greater discrepancies, which requires further investigation, in high velocity flows where the momentum of flow speed governs the process. It should also be noted that the proposed CA algorithm is particularly suitable for parallelization which would increase the computational power of the model and therefore the range of applications. The CA approach will be further developed to include both overland flow and the sewer network flow. The 2D CA model will be enhanced by including hydrological losses, e.g. infiltration. The methodology will be further improved to minimize the discrepancy and an investigation will be conducted into the relaxation parameters in detail so that they can be determined automatically. The model presented here might also be extended to incorporate the influence of buildings based on the concepts of BCR and CRF introduced in Chen *et al.* (2012a).

ACKNOWLEDGEMENTS

The authors would like to acknowledge the funding provided by the UK Engineering and Physical Sciences Research Council, grant GR/J09796 (Simplified Dual-Drainage Modelling for Flood Risk Assessment in Urban Areas). The authors would also like to thank the UK Environment Agency and the Ordnance Survey for providing the LiDAR and the Ordinance Survey Mastermap datasets.

REFERENCES

Chang, L. C., Shen, H. Y., Wang, Y. F., Huang, J. Y. & Lin, Y. T. 2010 Clustering-based hybrid inundation model for forecasting flood inundation depths. *Journal of Hydrology* **385**, 257–268.

Chen, A. S., Djordjević, S., Leandro, J. & Savić, D. 2007 The urban inundation model with bidirectional flow interaction between 2D overland surface and 1D sewer networks. NOVATECH 2007, 24–28 June 2007. Lyon, France, pp. 465–472.

Chen, A. S., Djordjević, S., Leandro, J. & Savić, D. A. 2010 An analysis of the combined consequences of pluvial and fluvial flooding. *Water Science and Technology* **62**, 1491–1498.

Chen, A. S., Evans, B., Djordjević, S. & Savić, D. A. 2012a A coarse-grid approach to representing building blockage effects in 2D urban flood modelling. *Journal of Hydrology* **426**, 16.

Chen, A. S., Evans, B., Djordjević, S. & Savić, D. A. 2012b Multi-layered coarse grid modelling in 2D urban flood simulations. *Journal of Hydrology* **470–471**, 1–11.

Coulthard, T. J., Macklin, M. G. & Kirkby, M. J. 2002 A cellular model of Holocene upland river basin and alluvial fan evolution. *Earth Surface Processes and Landforms* **27**, 269–288.

Crossley, A. J., Wright, N. G. & Whitlow, C. D. 2003 Local time stepping for modeling open channel flows. *Journal of Hydraulic Engineering – ASCE* **129**, 455–462.

Department of Environment 1981 *Design and Analysis of Urban Storm Drainage: The Wallingford Procedure*. National Water Council, London.

Dottori, F. & Todini, E. 2011 Developments of a flood inundation model based on the cellular automata approach: testing different methods to improve model performance. *Physics and Chemistry of the Earth* **36**, 266–280.

Downloaded from http://iwaponline.com/jh/article-pdf/15/3/676/387056/676.pdf
by guest

Ermentrout, G. B. & Edelstein-Keshet, L. 1993 Cellular automata approaches to biological modeling. *Journal of Theoretical Biology* **160**, 97–133.

Hsu, M. H., Chen, S. H. & Chang, T. J. 2000 Inundation simulation for urban drainage basin with storm sewer system. *Journal of Hydrology* **234**, 21–37.

Hunter, N. M., Bates, P. D., Neelz, S., Pender, G., Villanueva, I., Wright, N. G., Liang, D., Falconer, R. A., Lin, B., Waller, S., Crossley, A. J. & Mason, D. C. 2008 Benchmarking 2D hydraulic models for urban flooding. *Proceedings of the Institution of Civil Engineers – Water Management* **161**, 13–30.

Hunter, N. M., Horritt, M. S., Bates, P. D., Wilson, M. D. & Werner, M. G. F. 2005 An adaptive time step solution for raster-based storage cell modelling of floodplain inundation. *Advances in Water Research* **28**, 975–991.

Ilachinski, A. 2001 *Cellular Automata: A Discrete Universe*. World Scientific, New Jersey.

Itami, R. M. 1994 Simulating spatial dynamics – cellular-automata theory. *Landscape and Urban Planning* **30**, 27–47.

Judi, D., Burian, S. & Mcpherson, T. 2011 Two-dimensional fast-response flood modeling: desktop parallel computing and domain tracking. *Journal of Computing in Civil Engineering* **25**, 184–191.

Judice, S. F., Barcellos, B. & Giraldi, G. A. 2008 A cellular automata framework for real time fluid animation. Brazilian Symposium on Computer Games and Digital Entertainment, Belo Horizonte – MG, Brazil, Belo Horizonte – MG, Brazil, pp. 169–176.

Krupka, M., Pender, G., Wallis, S., Sayers, P. B. & Marti, J. M. 2007 A rapid flood inundation model. Thirty-second IAHR Congress, 2007, Venice, Italy, pp. 1–6.

Lamb, R., Crossley, M. & Waller, S. 2009 A fast two-dimensional floodplain inundation model. *Proceedings of the Institution of Civil Engineers – Water Management* **162**, 363–370.

Lhomme, J., Sayers, P. B., Gouldby, B. P. S. & Marti, J. M. 2008 Recent developments and application of a rapid flood spreading method. *European Conference on Flood Risk Management: Research and Practice*. Taylor and Francis, Oxford.

Maksimović, C., Prodanović, D., Boonya-Aroonnet, S., Leitao, J. P., Djordjević, S. & Allitt, R. 2009 Overland flow and pathway analysis for modelling of urban pluvial flooding. *Journal of Hydraulic Research* **47**, 512–523.

Neal, J., Fewtrell, T. & Trigg, M. 2009 Parallelisation of storage cell flood models using OpenMP. *Environmental Modelling and Software* **24**, 872–877.

Nguyen, D. K., Shi, Y. E., Wang, S. S. Y. & Nguyen, H. 2006 2D shallow-water model using unstructured finite-volumes methods. *Journal of Hydraulic Engineering – ASCE* **132**, 258–269.

Thomas, R. & Nicholas, A. P. 2002 Simulation of braided river flow using a new cellular routing scheme. *Geomorphology* **43**, 179–195.

Vojinovic, Z. & Tutulic, D. 2009 On the use of 1D and coupled 1D–2D modelling approaches for assessment of flood damage in urban areas. *Urban Water Journal* **6**, 183–199.

Wright, N. G., Whitlow, C. D. & Crossley, A. J. 1999 Locally adapted time steps for open channel flow with transitions. Twenty-eighth Congress of the IAHR, 1999, Austria, pp. 364–369.

Zhang, X. D., Trepanier, J. Y., Reggio, M. & Camarero, R. 1994 Time-accurate local time stepping method based on flux updating. *The American Institute of Aeronautics and Astronautics Journal* **32**, 1926–1929.

First received 5 March 2012; accepted in revised form 21 November 2012. Available online 27 December 2012

Downloaded from http://iwaponline.com/jh/article-pdf/15/3/676/387056/676.pdf
by guest